AN APPLICATION OF AN ENHANCED STATIONARY PHASE METHOD (SPM) APPROXIMATION FOR THE ASYMPTOTIC CALCULATION OF THE SCATTERED ELECTRIC FIELD FROM A FINITE RECTANGULAR PLATE

**Ch. G. Moschovitis, E. G. Papkelis, H. T. Anastassiu, K. T. Karakatselos,
I. Ch. Ouranos and P. V. Frangos**

*National Technical University of Athens, School of Electrical and Computer Engineering,
Division of Information Transmission Systems and Materials Technology,
Radar Systems and Remote Sensing Laboratory,
9 Iroon Polytechniou Str. 15773 Zografou, Athens, Greece
phone: +30210-772-3694 ;fax: +30210-772-2281;
e-mail: pfrangos@central.ntua.gr*

Abstract

Propagation in an urban outdoor environment which consists of three dimensional scatterers (walls) is the main goal of our research. Provided that both transmitter and receiver are located below rooftop level, this scenario pertains to propagation circumstances related to modern high frequency communication wireless networks. Such environment could be modeled through the prerequisite problem of an electromagnetic (EM) wave which is assumed to be incident on a perfectly conducting rectangular plate of finite dimensions.

Our contribution to the problem is a simulation application, which is based on an enhanced Stationary Phase Method asymptotic approximation for the calculation of the scattered electric field from a finite rectangular plate.

Our principal result is an SPM formula which produces thorough results analytically proven to correspond to a plane wave. The novel, important feature of our approach is the inclusion of the edge contribution to the resulting asymptotic expressions using – simple to implement, yet complicated in terms of results - improved edge contribution forms, which have not been documentted in the literature for the case of a double integral.

Simulation results are compared to results obtained with standard numerical integration, though SPM divulged here is incomparably faster.

1. Introduction

Let us consider the observation point Rx(x,y,z) in a propagation problem layout of an electromagnetic (EM) wave with wavevector k_i, which is assumed to be incident on a perfectly conducting rectangular plate of finite dimensions.
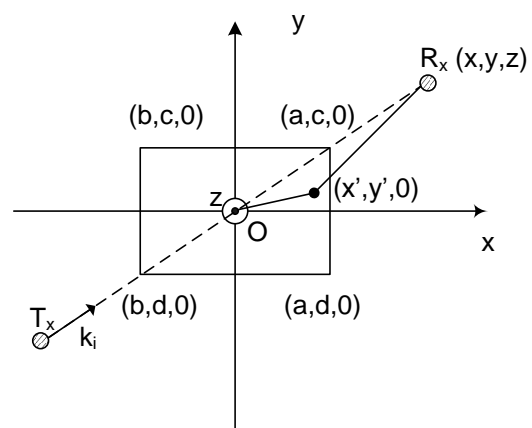
Figure 1. 3D geometry xy plane projection

This three dimensional scatterer is the necessary prerequisite in order to model propagation in an urban outdoor environment, which consists of three dimensional walls and obstacles that often pertain to modern high frequency

communication wireless networks, such as GSM, UMTS, Wi-Fi and Wi-Max technologies. Should the rectangular plate lie on the xy plane, two different approaches are distinguished according to the polarization of the incident field (TE + TM polarization).

2. Vector Potential $\bar{A}$ and Scattered Electric Field $\bar{E}$

According to P.O theory, the current density is equal to Eq. 1:

$$\bar{J}_s^{P.O} = 2 \cdot n \times \bar{H}_i \big|_{\substack{z=0 \\ y=y'}} = \hat{x} \cdot 2 \cdot \frac{E_0}{\eta} \cdot \cos \vartheta_i \cdot$$
$$\cdot \exp\left[- j \cdot k \cdot y' \cdot \sin \vartheta_i \right] \quad (1)$$

By utilising the three dimensional Green function (Eq. 2):

$$G(r,r') = \frac{\exp\left(- j \cdot k \cdot |r - r'|\right)}{4\pi \cdot |r - r'|} \quad (2)$$

the vector potential $\bar{A}$ at the observation point $R_x(x,y,z)$ is given by Eq. 3:

$$\underline{A}(x,y,z) = \mu_0 \cdot \int_{y'=d}^{c} \int_{x'=b}^{a} \left[\bar{J}_s^{P.O}(x',y') \cdot G(r,r') \right] \cdot dx' dy' \quad (3)$$

Substitution of total current density yields the potential vector expression (Eq. 4) for both TE and TM polarization:

$$\underline{A}(x,y,z) = \frac{-\mu_0}{2\pi \cdot \eta} \cdot$$
$$[\hat{x} \cdot (E_{0\theta} \cdot \cos \phi_i - E_{0\phi} \cdot \cos \theta_i \cdot \sin \phi_i) +$$
$$+ \hat{y} \cdot (E_{0\theta} \cdot \sin \phi_i + E_{0\phi} \cdot \cos \theta_i \cdot \cos \phi_i)] \cdot$$
$$\cdot \int_{y'=d}^{c} \int_{x'=b}^{a} \frac{\exp\left\{ j \cdot k \left[\begin{array}{c} (x'\cdot K + y'\cdot L) - \\ - \sqrt{(x-x')^2 + (y-y')^2 + z^2} \end{array} \right] \right\}}{\sqrt{(x-x')^2 + (y-y')^2 + z^2}} dx' dy' \quad (4)$$

since it is easily obtained from Fig. 1 that

$$|\underline{r} - \underline{r}'| = \sqrt{(x-x')^2 + (y-y')^2 + z^2} \quad (5)$$

and K, L constants which depend on the incident angles θ_i and ϕ_i satisfying Eqs. 6-7:

$$K = \sin \theta_i \cdot \cos \phi_i \quad (6)$$
$$L = \sin \theta_i \cdot \sin \phi_i \quad (7)$$

Finally the scattered electric field is calculated from the formula:

$$\underline{E}_s(x,y,z) = -j \cdot \omega \cdot \underline{A} - j \cdot \frac{\omega}{k^2} \cdot grad\left(div\left(\underline{A}\right)\right) \quad (8)$$

3. SPM approximations

Operating at the frequency of 1GHz or higher, scatterers that appear in the above networks are considered to be electrically large, and current density may be calculated with good accuracy using the physical optics (P.O.) approximation. Modifying appropriately Eq. 4 we can apply SPM approximations which result in calculating the vector potential and eventually the total scattered electric field at the observation point $R_x(x,y,z)$. The functions we use are derived in Eqs. 9-10:

$$F(x',y') = \frac{1}{\sqrt{(x-x')^2 + (y-y')^2 + z^2}} \quad (9)$$

$$f(x',y') = x'K + y'L - \\ - \sqrt{(x-x')^2 + (y-y')^2 + z^2} \quad (10)$$

The novel, important feature of our approach is the inclusion of the edges contribution to the resulting asymptotic expressions, which has not been documented in the literature for a double integral. In some cases [1] a literature approach for the solution of the above problem cannot be applied. This solution is achieved by inserting a rotation of the three dimensional system using spherical coordinates variables, resulting in rather complicated formulas which are not easy to neither handle,

nor implement or utilize in a modern propagation simulation tool. Additionally, the results of this rotation, due to the extreme complexity of the analytical values they include, are unable to produce an effective series of fast and adequate results.
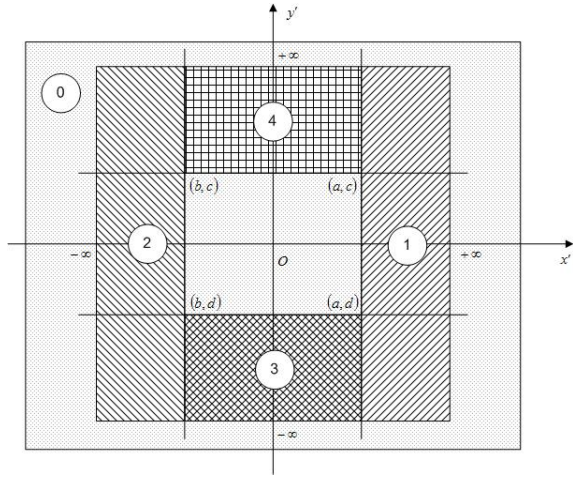
Figure 2. SPM approach

Our approach is illustrated in Fig. 4. According to this procedure, the initial integral, which is to be computed, is extended to infinite for both x' and y' variables. This extension primarily enables us to utilize the standard SPM formulas, documented for an infinite integral [2]. Since the plate is finite, additional correction terms should be included in the final SPM result. Those terms are obtained by subtracting the remaining areas around the finite plate. For those terms, the results are computed by utilizing a combination of SPM and edge contribution side formulas, thoroughly documented but only for the case of a single integral. By applying such calculations twice, we present here new functions on which we re-apply SPM approximations, and finally result in avoiding the complicated variable rotation and making the solution applicable. Using this technique we are also able to present thorough analytical results, which for the case of the double integral are really complicated. Eqs. 11-37 present the method explained above:

$$I(k) = \int_{y'=d}^{c} \int_{x'=b}^{a} F(x',y') \cdot e^{j \cdot k \cdot f(x',y')} dx' \cdot dy' =$$

$$\int_{-\infty}^{+\infty} \int_{-\infty}^{+\infty} F(x',y') \cdot e^{j \cdot k \cdot f(x',y')} dx' \cdot dy' - \int_{-\infty}^{+\infty} \int_{x'=a}^{+\infty} F(x',y') \cdot e^{j \cdot k \cdot f(x',y')} dx' \cdot dy' -$$

$$- \int_{-\infty}^{+\infty} \int_{-\infty}^{x'=b} F(x',y') \cdot e^{j \cdot k \cdot f(x',y')} dx' \cdot dy' - \int_{-\infty}^{y'=d} \int_{x'=b}^{a} F(x',y') \cdot e^{j \cdot k \cdot f(x',y')} dx' \cdot dy' -$$

$$- \int_{y'=c}^{+\infty} \int_{x'=b}^{a} F(x',y') \cdot e^{j \cdot k \cdot f(x',y')} dx' \cdot dy' \Rightarrow$$

$$I(k) = I[0] - I[1] - I[2] - I[3] - I[4] \tag{11}$$

$$I[0] = \int_{-\infty}^{+\infty} \int_{-\infty}^{+\infty} F(x',y') \cdot \exp(j \cdot k \cdot f(x',y')) \cdot dx' \cdot dy' =$$

$$= F(x_s,y_s) \cdot \frac{j \cdot 2 \cdot \pi \cdot \delta}{k \cdot \sqrt{|4A \cdot B - C^2|}} \cdot \cdot \exp(j \cdot k \cdot f(x_s,y_s)) \tag{12}$$

where

k: real number, relatively high.

x_s, y_s: Stationary points of f, i.e. the points for which both the partial derivatives of f in respect to x' and y' variables are zero.

$$\left. \frac{\partial f}{\partial x'} \right|_{\substack{x=x_s \\ y=y_s}} \equiv f'_{x'}(x_s,y_s) = 0 \tag{13}$$

$$\left. \frac{\partial f}{\partial y'} \right|_{\substack{x=x_s \\ y=y_s}} \equiv f'_{y'}(x_s,y_s) = 0 \tag{14}$$

f(x,y): Slow varying, real, non-linear function, independent of k.

F(x,y): Non-linear function, may be complex, but should also be independent of k.

a, b, c, d: Limits of double integral. The information of the limits is included in the location of stationary points x_s, y_s.

A, B, C: Constants related to the derivatives of function f which are calculated from Eqs. 15-17:

$$A = \frac{1}{2} \cdot f''_{xx}(x_s,y_s) \tag{15}$$

$$B = \frac{1}{2} \cdot f''_{yy}(x_s,y_s) \tag{16}$$

$$C = f''_{xy}(x_s,y_s) \tag{17}$$

δ: Value of δ is defined from the relative values of A, B, C constants:

$$\delta = \begin{cases} +1 & , \quad 4A \cdot B > C^2, A > 0 \\ -1 & , \quad 4A \cdot B > C^2, A < 0 \\ -j & , \quad 4A \cdot B < C^2 \end{cases} \quad (18)$$

$$I[1] = \int\limits_{-\infty}^{+\infty} \int\limits_{x'=a}^{+\infty} F(x', y') \cdot e^{j \cdot k \cdot f(x', y')} dx' \cdot dy' =$$

$$= \sqrt{\frac{2 \cdot \pi}{k \cdot \left| \dfrac{\partial^2 f'_{(02)}}{\partial y'^2} \right|_{y'=y_{02}}}} \cdot F'_{(02)}(y_{02}) \cdot$$

$$\cdot \exp\left(j \left[k \cdot f'_{(02)}(y_{02}) + \frac{\pi}{4} \cdot \mathrm{sgn}\left\{ \frac{\partial^2 f'_{(02)}}{\partial y'^2} \Big|_{y'=y_{02}} \right\} \right] \right)$$

$$(19)$$

$$I[2] = \int\limits_{-\infty}^{+\infty} \int\limits_{-\infty}^{x'=b} F(x', y') \cdot e^{j \cdot k \cdot f(x', y')} dx' \cdot dy' =$$

$$= \sqrt{\frac{2 \cdot \pi}{k \cdot \left| \dfrac{\partial^2 f'_{(03)}}{\partial y'^2} \right|_{y'=y_{03}}}} \cdot F'_{(03)}(y_{03}) \cdot$$

$$\cdot \exp\left(j \left[k \cdot f'_{(03)}(y_{03}) + \frac{\pi}{4} \cdot \mathrm{sgn}\left\{ \frac{\partial^2 f'_{(03)}}{\partial y'^2} \Big|_{y'=y_{03}} \right\} \right] \right)$$

$$(20)$$

$$I[3] = \int\limits_{-\infty}^{y'=d} \int\limits_{x'=b}^{a} F(x', y') \cdot e^{j \cdot k \cdot f(x', y')} dx' \cdot dy' =$$

$$= \int\limits_{-\infty}^{y'=d} (I'_0 - I'_a - I'_b) \cdot dy' =$$

$$= I[3.1] - I[3.2] - I[3.3]$$

$$(21)$$

$$I[3.1] = \int\limits_{-\infty}^{y'=d} I_o \cdot dy' = \frac{1}{jk} \cdot \frac{F'_{(01)}(d)}{\dfrac{\partial f'_{(01)}}{\partial y'} \Big|_{y'=d}} \cdot \exp\{jk \cdot f'_{(01)}(d)\}$$

$$(22)$$

$$I[3.2] = \int\limits_{-\infty}^{y'=d} I_a \cdot dy' = \frac{1}{jk} \cdot \frac{F'_{(02)}(d)}{\dfrac{\partial f'_{(02)}}{\partial y'} \Big|_{y'=d}} \cdot \exp\{jk \cdot f'_{(02)}(d)\}$$

$$(23)$$

$$I[3.3] = \int\limits_{-\infty}^{y'=d} I'_b \cdot dy' = \frac{1}{jk} \cdot \frac{F'_{(03)}(d)}{\dfrac{\partial f'_{(03)}}{\partial y'} \Big|_{y'=d}} \cdot \exp\{jk \cdot f'_{(03)}(d)\}$$

$$(24)$$

$$I[4] = \int\limits_{y'=c}^{+\infty} \int\limits_{x'=b}^{a} F(x', y') \cdot e^{j \cdot k \cdot f(x', y')} dx' \cdot dy' =$$

$$= \int\limits_{y'=c}^{+\infty} (I'_o - I'_a - I'_b) \cdot dy' = \quad (25)$$

$$= I[4.1] - I[4.2] - I[4.3]$$

$$I[4.1] = \int\limits_{y'=c}^{+\infty} I'_o \cdot dy' = -\frac{1}{jk} \cdot \frac{F'_{(01)}(c)}{\dfrac{\partial f'_{(01)}}{\partial y'} \Big|_{y'=c}} \cdot \exp\{jk \cdot f'_{(01)}(c)\}$$

$$(26)$$

$$I[4.2] = \int\limits_{y'=c}^{+\infty} I'_a \cdot dy' = -\frac{1}{jk} \cdot \frac{F'_{(02)}(c)}{\dfrac{\partial f'_{(02)}}{\partial y'} \Big|_{y'=c}} \cdot \exp\{jk \cdot f'_{(02)}(c)\}$$

$$(27)$$

$$I[4.3] = \int\limits_{y'=c}^{+\infty} I'_b \cdot dy' = -\frac{1}{jk} \cdot \frac{F'_{(03)}(c)}{\dfrac{\partial f'_{(03)}}{\partial y'} \Big|_{y'=c}} \cdot \exp\{jk \cdot f'_{(03)}(c)\}$$

$$(28)$$

Final results are obtained when substituting functions included in Eqs. 19-28 with the corresponding expressions using Eqs. 29-34, listed below:

$$F'_{(01)}(y') = \sqrt{\frac{2\pi}{k \left| \dfrac{\partial^2 f}{\partial x'^2} \right|_{x'=x_o, y'=y'}}} F(x_o, y') \cdot$$

$$(29)$$

$$\cdot \exp\left(j \cdot \frac{\pi}{4} \mathrm{sgn}\left\{ \frac{\partial^2 f}{\partial x'^2} \Big|_{x'=x_o, y'=y'} \right\} \right)$$

$$f'_{(01)}(y') = f(x_o, y') \quad (30)$$

$$F'_{(02)}(y') = -\frac{1}{jk} \cdot \frac{F(a, y')}{\dfrac{\partial f}{\partial x'} \Big|_{x'=a, y'=y'}} \quad (31)$$

$$f'_{(02)}(y') = f(a, y') \quad (32)$$

$$F'_{(03)}(y') = \frac{1}{jk} \cdot \frac{F(b, y')}{\dfrac{\partial f}{\partial x'} \Big|_{x'=b, y'=y'}} \quad (33)$$

$$f'_{(03)}(y') = f(b, y') \quad (34)$$

Equations I[1], I[2], I[3.1] and I[4.1] include the stationary points x_0 and y_{02}, y_{03} respectively. Since these integral terms refer to modified stationary points, as shown in Eqs. 35-37 below, their contribution will be included in the final result, only if these points are located between [c,d] and [b,a] respectively. In any other case, the contribution of these integral terms is zero.

$$\left.\frac{\partial f\left(x',y'\right)}{\partial x'}\right|_{x'=x_o,y'=y'} = 0 \qquad (35)$$

$$\left.\frac{\partial f'_{(02)}\left(y'\right)}{\partial y'}\right|_{y'=y_{02}} = 0 \qquad (36)$$

$$\left.\frac{\partial f'_{(03)}\left(y'\right)}{\partial y'}\right|_{y'=y_{03}} = 0 \qquad (37)$$

4. Simulation Results

Furthermore, in order to check the accuracy of our asymptotic calculations, standard (e.g. Gaussian) numerical integration was used to compare the results. Due to the complexity of the functions on which SPM is applied, the calculations were carried out using MATLAB's symbolic toolbox. A simulating application was also developed for the asymptotic SPM calculations. Results derived from MATLAB calculations constitute an aggregation of complicated formulas. Assuming an appropriate set of simulation parameters, the total electric field was calculated for distances in the Far Field, Fresnel Region and Near Field area. We compared SPM method and numerical integration for the frequency of 1GHz and for rectangular plates with side length equal to 20λ, 40λ, 60λ and 80λ. Both the elevation and azimuth angles of incidence were assumed equal to 45 degrees.

Comparison charts in Figs. 3 – 8 above indicate reasonable convergence between the asymptotic results of the SPM method, drawn with solid line, and

the numerical results of standard integration, drawn with dashed line.

4.1. Small Scatterer

In Figs. 3 – 5, numerical results are shown for a rectangular plate of side dimension 20λ in the Near Field area (r=25m), the Fresnel area (r=100m) and the Far Field area (r=300m).
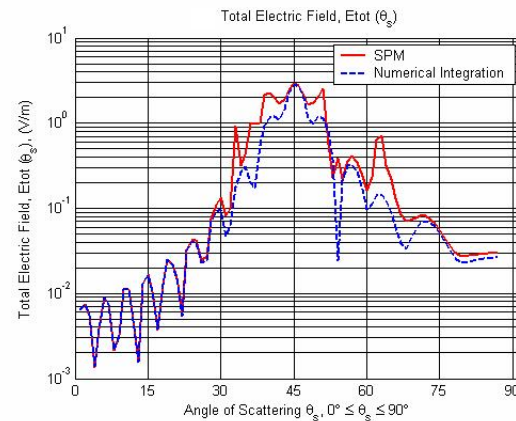
Figure 3. 20λ plate side, Near Field area
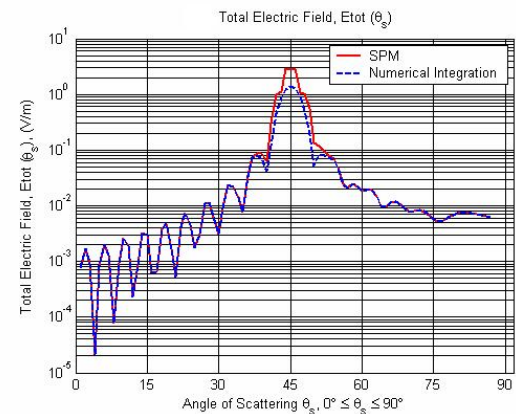
Figure 4. 20λ plate side, Fresnel area
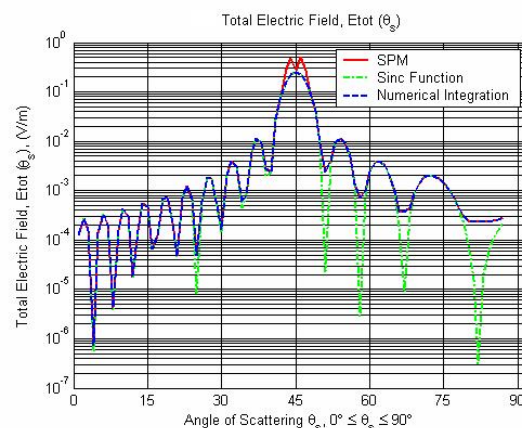
Figure 5. 20λ plate side, Far Field area

4.2. Large Scatterer

In Figs. 6 – 8, we provide results for the case of a larger scatterer of side dimension 80λ in the Near Field area
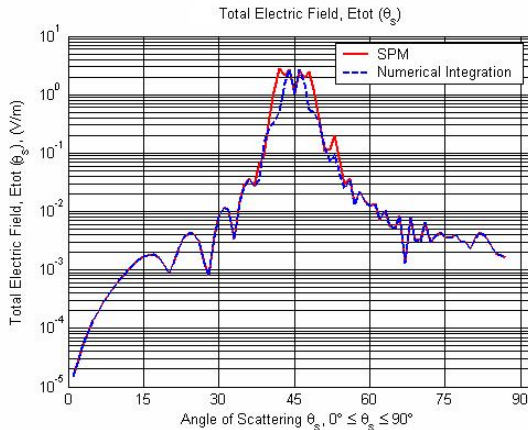
Figure 6. 80λ plate side, Near Field area
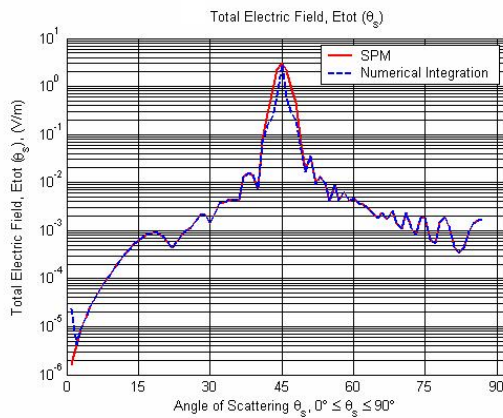
Figure 7. 80λ plate side, Fresnel area
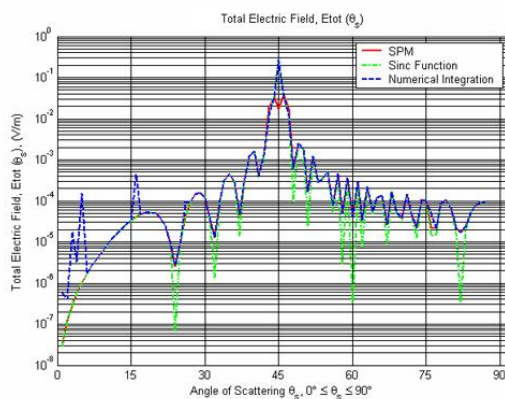
Figure 8. 80λ plate side, Far Field area

(r=100m), the Fresnel area (r=1000m) and the Far Field area (r=4500m).

These numerical results show satisfactory agreement between the two methods of computation for both cases of 20λ plate side and 80λ plate side scatterers. Deviations of the main lobe, which occur in the far field area only for both 20λ and 80λ plate side scatterers, are justified by the behaviour of Eqs. 22-24 and Eqs. 25-27.

5. Conclusion

Even though rather complicated mathematical formulas are involved in the proposed SPM method, it is very important that this technique is much faster than the numerical integration. Namely, SPM in this case is about 40 times faster. We can very easily understand how important this is for the numerical implementation of a simulated propagation problem in an urban outdoor environment, in which case many scatterers (walls) and multiple reflection phenomena are present. Furthermore, by increasing the dimensions of the scatterer, we are effectively increasing the frequency, thus reducing the error. The SPM method presented here appears to be very attractive for the calculation of vector potential $\vec{A}$ and electric field $\vec{E}$ in various radio propagation simulation tools.

Future development includes amelioration of the behaviour of the main lobe by reducing the errors using additional factorial integration.

References

[1] Graeme L. James, Geometrical Theory Of Diffraction for Electromagnetic Waves, UK, IEE 1976, pp. 30-42.

[2] C. A. Balanis, "Antenna Theory: Analysis and Design", John Wiley & Sons, NY, 1996, pp. 922-926.

[3] C. A. Balanis, "Advanced Engineering Electromagnetics", John Wiley & Sons, NY, 1989, pp. 586 -594.

[4] David C. Jenn, Radar and Laser Cross Section Engineering, American Institute of Aeronautics and Astronautics, Inc. Washington, 1995, pp. 29-33.